EXPERIMENTAL INVESTIGATION ON SYNTHETIC FIBER REINFORCED CONCRETE FILLED STEEL TUBE STUBS

K.Sai Krishna, *Post Graduate student, MGIT, Hyderabad*

S.Jayaprakash Narayana*, Assistant Professor, MGIT, Hyderabad*

Abstract: Concrete filled steel tube(CFST) columns are having higher ultimate load carrying capacity than conventional RC columns.CFST columns can be used in high rise buildings. Generally high strength concrete is used as a filling material in CFST columns. Due to the confinement of steel tube the load carrying capacity will be increased. In RC columns there is an improvement of load carrying capacity and ductility in presence of synthetic fibers. In this connection an attempt is required to find the role of synthetic fibers in CFST columns behavior.

In the present work an investigation was carried out to find the behavior of concrete filled steel tubes by varying thickness of steel tube and varying with synthetic fibers. In this work four different aspect ratios ((height to diameter), 1,2,3 and 4) of columns were tested with two different synthetic fiber ratios (0.5% and 1% of volume fraction). The experimental investigations were carried by using concrete grades M30. From the experimental results the effect of synthetic fibers on behavior on ultimate load carrying capacity of CFST columns was studied. The study shows, as the thickness of steel tube increases the load carrying capacity increases.

I.INTRODUCTION

CFS (concrete-filled steel) tubes are popular in multi-story structures because they favor economy and structural action. It improves not only the load-carrying capacity of the section but also ductility and energy absorption (Ho, (2014), Charles (2010)). The improvement of capacity is due to the confinement of the concrete core; also, the steel tube acts as longitudinal reinforcement. Due to this, the section dimensions can be reduced up to 30% compared to conventional reinforced concrete sections. This type of column can be used in high-rise structures, bridges, suspension bridges, electricity cables supporting poles etc.

Different CFS tube cross-sections can be adopted. The most commonly used circular and square hollow sections filled with concrete. The corners are made fillet for square sections to avoid stress concentration, as shown in Fig.1.1. The types of CFS tube includes double skin concrete-filled steel tubes (DSCFST) (Fig 1.2a), encases a section roller sections in CFST column (Fig 1.2b), providing additional reinforcement in the CFST column (Fig 1.2c) and stiffened CFST columns (Fig 1.2d).

CFS tube columns offer economical and rapid construction. Because the steel tube acts as a formwork, no separate formwork is required for CFStube columns. The steel tube also acts as a longitudinal reinforcement to the columns. Erecting the steel tube takes less time to fix the formwork for the RC column, making it economical and simple construction. Conventional concrete may have the problem of vibration for CFS tube columns. This can be overcome by using self-compacting concrete (Charles (2010)).

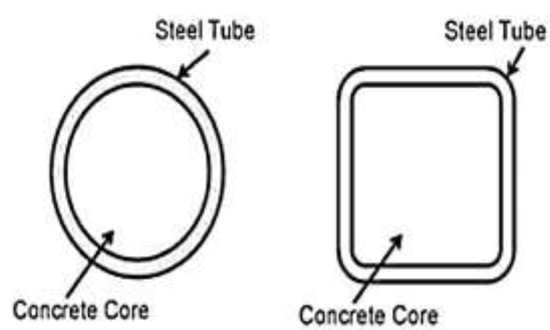

Fig 1.1: circular and square cross section of CFS tubes

1.1 Advantages of CFS tube columns

The following are the advantages of CFS tube columns

1. It improves the load-carrying capacity of the column compared to RC columns
2. The outer tube acts like a longitudinal reinforcement
3. The ductility of the combined section will be improved.
4. 10 to 30% of material will be saved due to a reduction in sizes of sections.
5. Inelastic deformation of the section will be improved.
6. Separate formwork is not necessary since the tube itself acts like formwork.
7. The time of the construction will be reduced.
8. Provides better aesthetic appearance.

Despite above advantages, there are some shortcomings, like the interface between steel concrete. At the loading's elastic stage, the steel tube dilates higher than the concrete (Uy, 2001), which decreases the stiffness of the member.

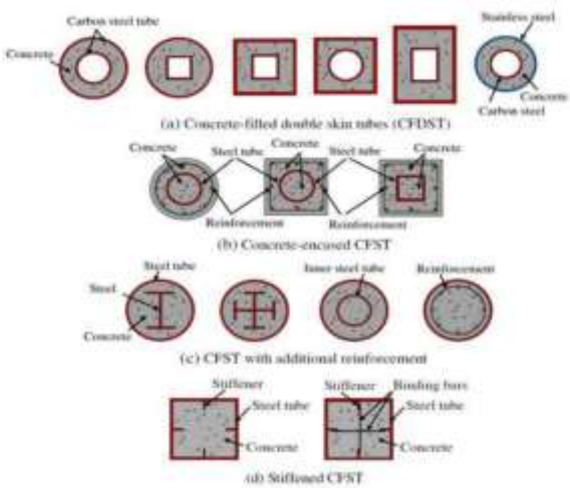

Fig 1.2: Various types of CFS tube cross sections

Fig 1.3: Application of CFST columns in buildings

Fig 1.4: Application of CFST column as a powerline pole

1.2 Behaviour of CFS tube columns

The load-carrying capacity of the CFS tube column increases over RCC column due to the confinement concrete offered by the steel tube. The confinement starts only when the micro-cracking starts in concrete. At this point, the concrete reaches the maximum value of Poisson's ratio. Consequently, it dilates more and immediately confining pressure activates by the steel tube e (Ferretti, 2004; Lu and Hsu, 2007).

Circular CFS tube columns offer more bond stress transfer than square CFS tube columns. Shear stress transfer and bond stress transfer are required to get the composite action. CFS tube columns fail in different modes. Some failure modes have shown in Fig 1.5a. The steel tube may undergo outward buckling due to less thickness of the steel tube under axial loads. If the concrete core fails by shear failure, then the failure may be as shown in Fig 1.5b. Due to the dilation of concrete, the concrete exerts outward pressure causing outward buckling of the tube as shown in Fig 1.5c.

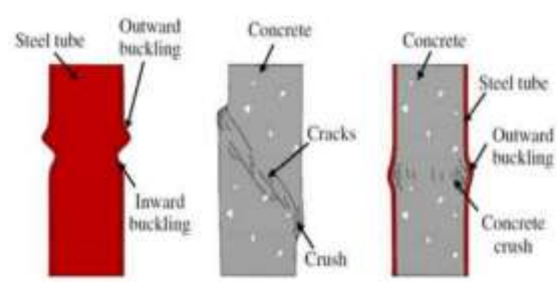

Fig 1.5: Different failure modes of CFS tube columns

1.3 Methodology:

The present study is planned for two stages. M20 grade of concrete mix proportions designed as per IS 10262:2019. Trial mixes were prepared and checked after 28 days. If the strength is not attained, corrections were made, trial mixes were again made and tested. The steel tubes were procured and cut desired heights, grinded, and leveled surfaces. In the first stage, the study planned to understand the thickness of steel tube thickness in CFS tube stubs. In the second phase of the study planned to understand the effect of fibers on CFS tube stubs

1.4 Objectives of the present study

1. To understand the effect of thickness on axial behaviour of CFS tube stubs

2. To acknowledge the effect of aspect ratio (height to diameter) for 3mm and 5mm thickness of concrete-filled steel tubes.

3. To understand the effect of synthetic fiber dosages of 0.5% and 1% on the behaviour of CFS tube stubs.

4. To observe the effect of aspect ratio for 0.5% and 1% of volume fraction of FRC filled with steel tubes.

II. LITERATURE REVIEW

Ramdinesh P et.al. (2018) worked on analytical studies of CFST which were wrapped with Kevlar polymer. In the study, 4 different specimens with and without Kevlar fibers analysied using FEM software. The specimens were in the form of tubes of 10 cm dia 50 cm height and thickness of tube 1cm. The deformations were evaluated and confirmed that bi-directional Kevlar fibers prolongs the deformations.

Keigo T et.al. (2000) conducted tests on sixty CFST beams columns of33 and 31 width/ diameter to thickness ratio were used. Cold-formed steel of square and circular columns was used. Different L/D ratios (4,8,12,18,24 and 30 also different eccentricities e=0,k,3k,5k (where k= core of section) were considered in the study. From the study, it was concluded that an L/D ratio of 4 gives conservative results.

Y. F. Zhang et. al. (2015) studied on analysis of composite action of concrete-filled steel tube columns reinforced by confining materials. Four different types of concrete-filled tubes were considered in the study. A hollow steel tube filled with concrete, a concrete-filled steel column, and a carbon tube filled with concrete. The unified theory was applied to calculate load capacity and matched experimental results.

III.EXPERIMENTAL PROGRAM

The CFS tube columns have advantages that include, an increase in load-carrying capacity and improve the post-peak behaviour. In the presence of fibers in RCC, the crack resistance and post-peak response of columns will improve. Therefore, in this study, the focus is on understanding the effect on the behaviour of CFS tube stubs and the effect of PO fibers on the behaviour of CFS tube stubs. The parameters considered, mix proportions, methodology of the project are explained in this chapter.

3.1 Methodology

The present work was carried out in two phases. In the first phase of the work, casting and testing were done on CFS tubes of 3 mm and 5 mm thickness. Four different height of specimens 100 mm, 200 mm, 300 mm, and 400 mm, were considered. The internal diameter of 100 mm tube was used. The material proportions are detailed in Table 3.1.

In the second phase of the work casting and testing done on CFS tube filled with FRC of 0.5% and 1% of volume fraction of PO fibers. Four different heights of specimens, 100 mm, 200 mm, 300 mm, and 400 mm, were considered. The internal diameter of the 100 mm tube was used. The material proportions were detailed in Table 3.1, and the mix design procedure is presented in Appendix 1. The properties of PO fibers supplied by the client are shown in Table 3.2. The carried-out work is represented schematically in Fig 3.1.

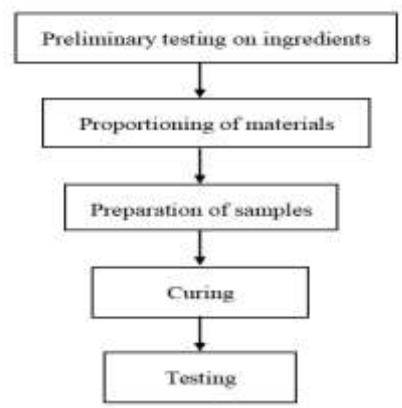

Fig: 3.1 Schematic view of stages of work

Table 3.1 : Mix proportions

Cement kg/ m^3	Fine aggregate kg/ m^3	Coarse aggregate kg/ m^3	Water lit/ m^3	S.P kg/ m^3	Average compressive strength (fck) N/ mm^2	0.5 % PO fibers kg/ m^3	1% PO fibers kg/ m^3
334.151	887.496	1093.523	143.685	6.683	25.4	4.55	9.1

3.2 Preliminary tests

Prior to mix design, the properties of the ingredients were found and tabulated in Table 3.2. All the results were obtained within the permissible limits. The properties of fibers are shown in Table 3.3.

Table 3.2 : Properties of ingredients

Property/material		**Obtained result**
Specific gravity	Cement	3.05
	Fine Aggregate	2.45
	Coarse aggregate	2.51
Standard consistency of cement		32%
Fineness of cement		7.5%

Table 3.3 : Specifications of Polyolefene fibers

Property	**Value of fiber**
Length (cm)	5
Diameter (cm)	0.05
Specific gravity	0.91
Tensile strength (N/mm^2)	618
Elastic modulus (N/mm^2)	10×10^3
Aspect ratio	100
Density (kg/m^3)	910

3.3 Casting of specimens

The material proportions were presented in Table 3.1 were taken and mixed in a concrete mixer. After mixing of concrete slump test was conducted to check the workability. The slump was obtained 70mm for the concrete without fibers. Whereas for the 0.5% volume fraction of PO fibers, it was 30 mm, and for 1% of PO fibers 15mm. For the second phase of the work, 5 mm thick tubes were used. The concrete was filled in the steel tubes, which were cut required height and surface was grind and level was checked. The steel tubes before cut were shown in Fig 3.2.

The concrete was filled in tubes for 3 layers for 100 mm and 200 mm height specimens and 4 layers for 300 mm and 400 mm height specimens. Each layer was compacted using tamping rad with 25 tamps. The top layer was finished with cement paste to get smooth surface. The prepared specimens were shown in Fig 3.3. A curing compound was applied on the top and bottom surface after 24 hours and kept specimens at ambient temperature. The specimens were covered with gunny bags. The curing compound was applied once a week.

Fig 3.2: Steel tube before cutting

Fig: 3.3 Preparation of specimens

After 28 days of curing, the specimens were tested under a compression testing machine of a capacity of 3000 kN. A dial gauge was mounted and noted deformations at different intervals to monitor the axial deformation, as shown in Fig 3.4. For the first phase of the study, semi-automatic CTM was used (Fig 3.4) whereas for the second phase of the study, servo-controlled CTM of 3000 kN (Fig 3.5) was used. In the second phase of the work, the axial deformation was directly taken from the stroke displacement stored through the data acquisition system.

In the first phase of the study, the experiments were continued up to 20 mm axial deformation as the limitation of the dial gauge.

Fig: 3.4 Testing of CFS stub in the first phase of the study

IV.RESULTS AND DISCUSSIONS

The present study focuses on understanding the effect of thickness of steel tube on behaviour of CFS stubs and effect of fibers on axial behaviour of CFS column. The experimentation was carried out in two phases. In the first phase of the work, casting and testing were done on CFS columns by varying steel tube thickness (3 mm and 5 mm). In the second phase of the work, casting, and testing of CFS, columns were done by varying fiber dosages (0.5% and 1%). Two dosages 0.5% and 1% of volume fractions of PO fibers, were considered with a tube thickness of 5 mm. In both the phases, the tube internal diameter was kept constant (100 mm), and the specimens' height was varied viz 100mm, 200 mm, 300 mm, and 400 mm. The experimental procedure is explained in 3.3. Based on the experiments, the results are presented in this chapter.

4.1 Phase I study

4.1.1 Results of CFS stubs with 3 mm thickness of tube

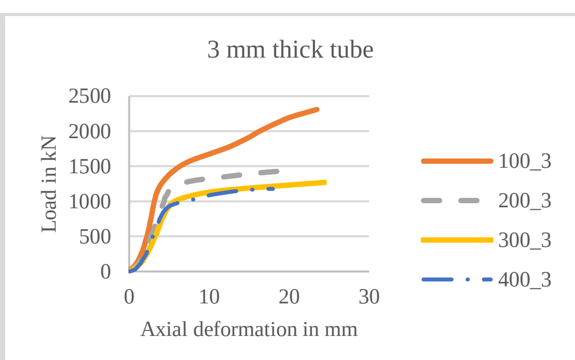

Fig 4.1: Load vs Axial deformation for 3 mm thickness specimen

Fig 4.1 shows the load vs axial deformation for 3 mm thickness specimens. It shows that as the height of the specimen increases, the load-carrying capacity decreases. In the 100 mm specimen, the buckling of tube shows more strain hardening behaviour than other specimens. In the 200 mm specimen the strain hardening behaviour is less compared to the 100 mm height specimen. The specimens of 300 mm and 400 mm height columns show almost the same behaviour, showing that the axial compression failure is dominated by buckling of the specimen. The initial stiffness of all the stubs is almost the same except in the 100 mm height specimen. The initial measurement may not be captured due to the inefficiency of machinery.

4.1.2 Results of CFS stubs with 5 mm thickness of tube

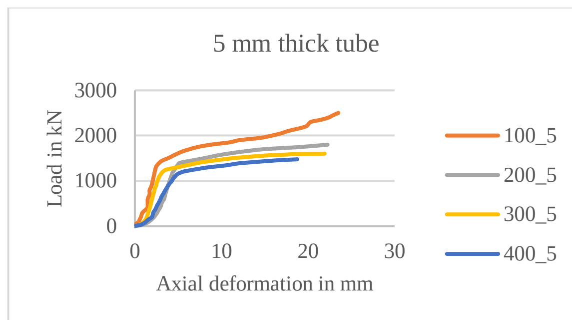

Fig 4.2: Load vs Axial deformation for 5mm thick CFS specimens

Fig 4.2 shows the load vs axial deformation for 5 mm CFS tube specimens. It shows that as the height of the specimen increases, the load-carrying capacity decreases. In the 100 mm specimen, after buckling of tube, it shows more strain hardening behaviour than other specimens. In the 200 mm specimen, the strain hardening behaviour is less compared to the 100 mm height specimen. The specimens of 300 mm and 400 mm height columns show almost the same behavior, showing that the axial compression failure is dominated by buckling of the specimen.

.4.1.3 Results of CFS stubs with 3 mm thickness of tube (300 height)

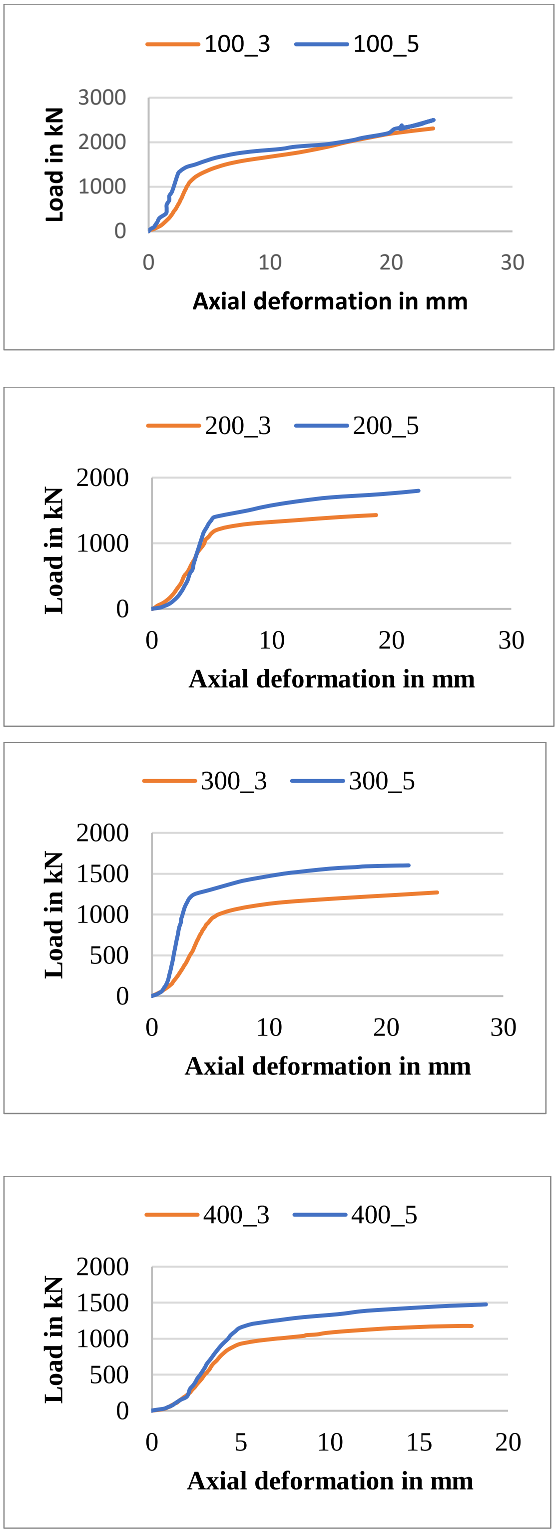

Fig 4.3: Comparision of 3mm and 5 mm specimens

Fig 4.3 shows the comparison of 3 mm and 5 mm CFS tubes of 100 mm, 200 mm, 300 mm and,400 mm height specimens. The initial stiffness is almost the same in all the specimens. The stiffness may differ due to the initial imperfection in the specimen. By comparing 3 mm and 5 mm tube, as the thickness of tube increases, the buckling capacity of the CFS tube increases along with the post-buckling stiffness.

4.1.4 Failure modes

Fig 4.4: Failed specimens of 3mm CFS tubes

Fig 4.4 and Fig 4.5 show the failure modes of the 3 mm and 5 mm CFS tube specimens respectively. It is observed that for the 100 mm height samples, the force was applied concentrically, whereas in other specimens, after specific loading due to the buckling of the specimen, the load was applied eccentrically. Specially, if the specimen had to buckle at ends, it tends to be eccentric, and in those specimens, the buckling is in the middle third height subjected to concentric loading. To avoid the end failure, it is necessary to strengthen at the ends of the specimens.

Fig 4.5: Failed specimens of 5mm CFS tubes

4.1.5 Overall behaviour

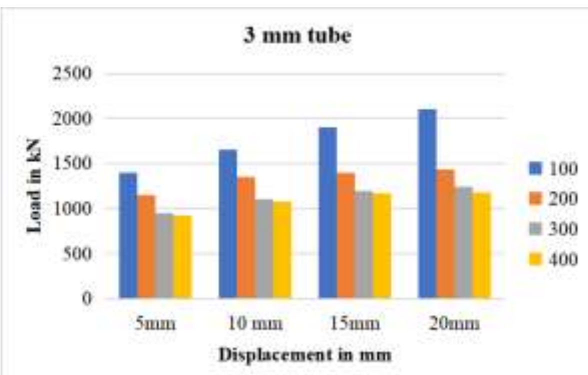

Fig 4.6: Comparison of Load values at different values of displacements in 3mm CFS tube specimens

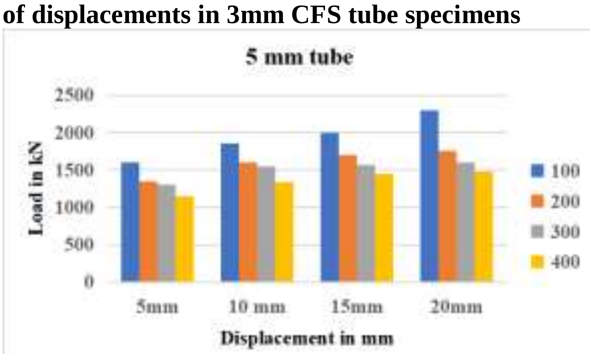

Fig 4.7: Comparison of Load values at different values of displacements in 5mm CFS tube specimens

Fig 4.6 and Fig 4.7 show the load values at different displacements in 3 mm and 5 mm CFS tube specimens. At 5 mm displacement in 5 mm thick specimens, there is a load decrement of 17% from 100 mm to 200 mm height specimens, whereas 32% and 34% decrement in 300 and 400 mm specimens, respectively. The 300- and 400-mm specimens load values are almost nearer at 10 mm,15 mm, and 20 mm displacements. In the case of 3 mm thick specimens, there is a load decrement of 15% from 100 mm to 200 mm height specimens, whereas 18% decrement in 300 mm height specimens and 28% in 400 mm height specimens. The loads at different displacements in 3 mm and 5 mm thick specimens follow similar trends. At 20 mm displacement, there is a significant decrement from 100 mm height to 200 mm height specimens, and the decrement is slight from 300 mm to 400 mm height specimens.

4.2 Phase II study

4.2.1 Results of CFS stubs with 0.5% volume fraction

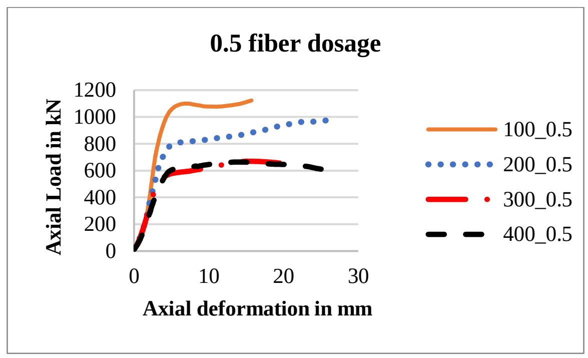

Fig 4.8: Load vs Axial deformation for 0.5% specimens

Figure 4.8 shows the load vs axial deformation for 0.5% of the volume fraction of CFS tube specimens. It shows that as the height of the specimen increases, the load-carrying capacity decreases. In the 100 mm and 200 mm specimens, the tube's buckling showed more strain hardening behaviour than other specimens. The specimens of 300 mm and 400 mm height columns show almost the same behavior, showing that the axial compression failure was dominated by buckling of the specimen. The initial stiffness of all the stubs is almost the same except in the 100 mm height specimen. The initial measurement may not be captured due to the inefficiency of machinery.

4.2.2 Results of CFS stubs with 1% volume fraction

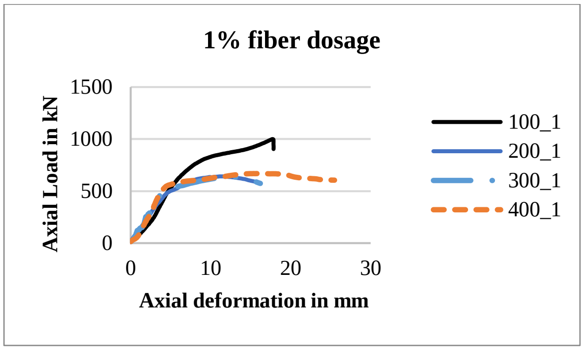

Fig 4.9: Load vs Axial deformation for 1% specimens

Figure 4.25 shows the load vs axial deformation for 1% volume fraction of CFS tube specimens. It shows that as the height of the specimen increases, the load-carrying capacity decreases. In the 100 mm specimen, the buckling of the tube shows more strain hardening behaviour than other specimens. The specimens 200 mm, 300 mm, and 400 mm height columns show almost the same behavior, showing that the axial compression failure is dominated by buckling of the specimen.

4.2.3 Failure modes

Fig 4.10 and Fig 4.11 show the failure modes of the 0.5%, 1% volume fraction CFS tube specimens, respectively. It is observed that for the 100 mm and 200 mm height samples, the force was applied concentrically, whereas in other specimens, after certain loading due to the buckling of the specimen, the load was applied eccentrically (Fig 4.30 (c)). Especially if the specimen had buckling at ends, it tends to be eccentric, and in those specimens, the buckling is in the middle third height subjected to concentric loading.

Fig 4.10: Failure modes of 0.5% fiber dosage specimens

To avoid the end failure, it is necessary to strengthen at the ends of the specimens. Some specimens show ruptures of steel tubes due to the excessive buckling in which, after maximum yielding, shown a softening behaviour (Fig .4.30 (a))

.

Fig 4.11: Failure modes of 1% fiber dosage specimens

V. CONCLUSIONS

An experimental investigation is carried out on concrete filled steel tubular (CFST) short column in two phases. In the first phase of the work, CFST stubs were tested to understand the effect of thickness on different aspect ratios of CFST stubs. The second phase of the work was carried out to understand the effect of fibers on the aspect ratio of CFST stubs. In the first phase of the work, two different thicknesses 3 mm and 5 mm, and four different aspect ratios (h/d) 1, 2, 3, and 4, are considered. In the second phase of the work, two different thicknesses fiber dosages of 0.5% and 1% volume fractions for four different aspect ratios (h/d) 1, 2, 3, and 4 are considered. M20 grade of concrete used for the study. The experimental results were presented and discussed in chapter 4. Based on the results, the conclusions are presented in this chapter.

5.1 Conclusions

1. As the thickness of the steel tube increases, the buckling load also increases. The buckling load increased by 7% in aspect ratio 1 specimen, 28%, and 23% in the aspect ratio of 2 and 3, respectively. Whereas in aspect ratio 4 the buckling load increased only 6%.

2. Providing higher fiber dosage will not help to improve the performance. The buckling load in 0.5% fiber dosage specimen increased by 33% in aspect ratio 1 specimen, 28% in the aspect ratio of 2, and negligible in aspect ratio 3 and 4 compared to 1% fiber dosage specimens. There is no significant effect of fibers at higher dosages.

References:

1. Charles W. Roeder, Dawn E. Lehman, and Erik Bishop, “Strength and Stiffness of Circular Concrete-Filled Tubes”, OURNAL OF STRUCTURAL ENGINEERING, ASCE / DECEMBER 2010 / 1545-1553.
2. Ferretti E (2004) On Poisson’s ratio and volumetric strain in concrete. International Journal of Fracture 126(3): 49–55.
3. Hasan Hastemoglu and İlker Erkan, “Behaviour of Double Skinned Composite Columns with Concrete Filled Tubular Column” J Archit Eng Tech, Volume 6, Issue 2, DOI: 10.4172/2168-9717.1000194
4. Ho, Lai and Luo, “Uniaxial behaviour of confined highstrength concrete-filled-steel-tube columns”, Structures and Buildings, Volume 167 Issue SB9, 2014
5. Hasan Hastemoglu and İlker Erkan, “Behaviour of Double Skinned Composite Columns with Concrete Filled Tubular Columns”, Journal of Architectural of Engineering Technology, 2017, 6:2 DOI: 10.4172/2168-9717.1000194
6. Iqbal Wahed, “Influence of Polyethylene Fiber and Super Plasticizer on The Properties of Fiber Reinforced Concrete”, A project presented to Ryerson University, Toronto, Ontario, Canada, 2016.
7. IS 10262 :2019, “Concrete Mix Proportioning — Guidelines”, Bureau of Indian Standards, New Delhi,2019
8. IS 456:2000, “Plain And Reinforced Concrete - Code Of Practice”, Bureau of Indian Standards, New Delhi,2000
9. Jingfeng Wanga,b , Qihan Shena, Fengqin Wanga , Wei Wang, “Experimental and analytical studies on CFRP strengthened circular thin walled CFST stub columns under eccentric compression” Thin-Walled Structures 127 (2018) 102–119
10. Kenji Sakino, Hiroyuki Nakahara, Shosuke Morino, and Isao Nishiyama, “Behavior of Centrally Loaded Concrete-Filled Steel-Tube Short Column”, J. Struct. Eng., 2004, 130(2): 180-188, Keigo TSUDA, Chiaki MATSUI, Eiji MINO, “Strength and Behavior of Slender Concrete Filled Steel Tubular Columns” 12WCEE 200.